tvst

Article

Validating Fluorescent Chrnb4.EGFP Mouse Models for the Study of Cone Photoreceptor Degeneration

Alicia A. Brunet[1,2], Paula I. Fuller-Carter[2], Annie L. Miller[1,2], Valentina Voigt[2], Sophia Vasiliou[2], Rabab Rashwan[2,3], David M. Hunt[1,2], and Livia S. Carvalho[1,2]

[1] Centre for Ophthalmology and Visual Sciences, The University of Western Australia, Nedlands, Western Australia, Australia
[2] Lions Eye Institute, Nedlands, Western Australia, Australia
[3] Department of Microbiology and Immunology, Faculty of Medicine, Minia University, Minia, Egypt

Correspondence: Livia S. Carvalho, Centre for Ophthalmology and Visual Sciences, The University of Western Australia, Nedlands, Western Australia, Australia. e-mail: liviacarvalho@lei.org.au

Received: May 1, 2020
Accepted: June 29, 2020
Published: August 18, 2020

Keywords: photoreceptors; retinal degeneration; cones; green fluorescent protein; Chrnb4.GFP

Citation: Brunet AA, Fuller-Carter PI, Miller AL, Voigt V, Vasiliou S, Rashwan R, Hunt DM, Carvalho LS. Validating fluorescent chrnb4.EGFP mouse models for the study of cone photoreceptor degeneration. Trans Vis Sci Tech. 2020;9(9):28, https://doi.org/10.1167/tvst.9.9.28

Purpose: To validate the application of a known transgenic mouse line with green fluorescent cones (Chrnb4.EGFP) to study cone photoreceptor biology and function in health and disease.

Methods: Chrnb4.EGFP retinas containing GFP$^+$ cones were compared with retinas without the GFP transgene via immunohistochemistry, quantitative real-time polymerase chain reaction, electroretinograms, and flow cytometry. The Chrnb4.EGFP line was backcrossed to the mouse models of cone degeneration, *Pde6c*^{cpfl1} and *Gnat2*^{cpfl3}, generating the new lines *Gnat2*.GFP and *Pde6c*.GFP, which were also studied as described.

Results: GFP expression spanned the length of the cone cell in the Chrnb4.EGFP line, as well as in the novel *Gnat2*.GFP and *Pde6c*.GFP lines. The effect of GFP expression showed no significant changes to outer nuclear layer cell death, cone-specific gene expression, and immune response activation. A temporal decrease in GFP expression over time was observed, but GFP fluorescence was still detected through flow cytometry as late as 6 months. Furthermore, a functional analysis of photopic and scotopic electroretinogram responses of the Chrnb4 mouse showed no significant difference between GFP$^-$ and GFP$^+$ mice, whereas electroretinogram recordings for the *Pde6c*.GFP and *Gnat2*.GFP lines matched previous reports from the original lines.

Conclusions: This study demonstrates that the Chrnb4.EGFP mouse can be a powerful tool to overcome the limitations of studying cone biology, including the use of this line to study different types of cone degeneration.

Translational Relevance: This work validates research tools that could potentially offer more reliable preclinical data in the development of treatments for cone-mediated vision loss conditions, shortening the gap to clinical translation.

Introduction

Inherited retinal degeneration (IRD) is a major contributor to early onset blindness worldwide, with an estimated incidence of 1:2000.[1] The recent advances in genetic therapy for IRD have provided exciting clinical and preclinical validation of novel treatments, but have also highlighted some of the existing knowledge gaps surrounding disease pathways, hindering the discovery of potential new therapeutic targets. Mutations in more than 250 genes are known to cause IRD, making it one of the most genetically diverse group of diseases (RetNet, https://sph.uth.edu/RetNet/).[2] IRDs do, however, share a key feature: progressive dysfunction and death of the light-sensing retinal photoreceptor cells. Cone photoreceptors, the photoreceptor cells responsible

Copyright 2020 The Authors

This work is licensed under a Creative Commons Attribution-NonCommercial-NoDerivatives 4.0 International License.

for daylight and high-acuity vision, are particularly susceptible to degeneration in IRD and other complex vision loss disorders such as age-related macular degeneration. IRD-causing mutations have been reported in genes that are either common to both photoreceptor types (cone-rod dystrophies) or specific to either rod or cone genes (rod or cone dystrophies, respectively).[3] Interestingly, cone photoreceptors seem appear to be particularly sensitive, with altered cone function and cone loss occurring even when the genetic lesion is present in a rod-specific gene. Despite cones being essential to maintain good quality vision, research into cone biology has lagged behind that of rods. This is largely because cones comprise a small percentage of the total number of cells in most mammalian retinas (3%–5% in the mouse and human retinas),[4] making it extremely difficult to study these cells in isolation.

Mouse models have become an invaluable tool for studying IRDs, as they allow for the in-depth analysis of functional, structural, and molecular changes of the retina in response to photoreceptor degeneration, offering unprecedented insight into retinal disease pathogenesis. Given the similarities in retinal physiology and visual processing function between humans and mice, several naturally occurring mutant and transgenic mouse models of IRD have been validated for studying disease mechanisms.[5] However, the lack of a concentrated cone photoreceptor population in the mouse retina, such as the macular region of the human retina, along with a 30:1 rod to cone ratio, has made the localization and visualization of cone photoreceptors in the mouse retina historically very challenging.

Several studies into the biology of cones in health and disease have relied on data from animal models of a disorder called achromatopsia, one of the few IRDs that affect cone photoreceptors exclusively.[6] Also referred to as rod monochromacy, achromatopsia is a devastating early onset disease estimated to affect 1:30,000 to 1:50,000 people worldwide.[7] Clinical symptoms start at birth/early infancy and include not only completely absent color discrimination with no recordable electroretinogram cone function, but also congenital pendular nystagmus, poor visual acuity, severe photophobia, and hemeralopia.[7,8] Mutations in six genes, specific to cones and essential for their function and development, have been reported to cause achromatopsia: *CNGA3*, *CNGB3*, *GNAT2*, *PDE6C*, *PDE6H*, and *ATF6*.[8]

In vivo retinal imaging has shown a highly variable range of cone photoreceptor integrity and structure between patients with achromatopsia, and, more important, it is variable between the genotypes.[9–11] Achromatopsia has been historically considered a stationary disease with absent cone function from birth, leading to the notion that cones in these patients did not undergo active degeneration throughout their lifetime.[12] However, several cross-sectional and longitudinal studies have reported disease progression over time mainly in *CNGA3* and *CNGB3* patients,[13–15] but also in *GNAT2*[15,16] and *PDE6C*.[17] Some of these studies indicate that there might be a higher rate of cone deterioration within the first years of life that then becomes stationary in older patients.[14,17] Indeed, gene rescue therapy studies have demonstrated the presence of an optimal treatment window in the *CNGB3*$^{-/-}$ mouse and dog models.[18,19] With five active clinical trials testing gene therapy treatments for achromatopsia (clinicaltrials.gov; NCT03278873, NCT03758404, NCT02935517, NCT02599922, and NCT02610582), understanding the differences in disease progression and varying levels of cone integrity and structure between genotypes will have crucial implications in the design and results of these trials.

To circumvent the problems associated with cone studies, researchers in the field were given an elegant solution a decade ago by Siegert et al. In this pivotal study, Siegert et al[20] analyzed the retina of 536 mouse lines created by The Gene Expression Nervous System Atlas project (GENSAT, The Rockefeller University, New York, NY).[21,22] Each of these lines express the green fluorescent protein (GFP) driven by different bacterial artificial chromosomes and their screening allowed for the identification of several mouse lines where retinal cell types were selectively labelled. One of these lines was the Chrnb4.EGFP line where the enhanced *GFP* (EGFP) gene was inserted upstream of the cholinergic receptor nicotinic beta 4 subunit (*Chrnb4*) gene, producing easily identifiable cone photoreceptors that exclusively express GFP throughout the entirety of the cone cell, from the outer segments to the synapse feet. This greatly facilitated cone visualization and isolation from the remaining retinal cellular population. Since its publication, the Chrnb4.EGFP mouse model has been used in only three cone-related studies.[23–25] The full potential of this novel transgenic mouse model as a research tool for the study of cone-related diseases has yet to be fully exploited, and very little is yet known about the expression of *Chrnb4* in the mouse retina in relation to the reliability of cone-specific GFP expression and any long-term effects on cone viability and function.

This study investigates the effects of GFP expression in the Chrnb4.EGFP mouse line on cone cell biology, including cone-specific gene expression and physiology, to evaluate the potential of this line as a

research tool to advance our understanding of cone biology and disease. It also describes two transgenic cone degeneration mouse lines created by crossing the Chrnb4.EGFP line with two previously described[26–28] mouse models of achromatopsia, the *Pde6c*^{cpfl1} and the *Gnat2*^{cpfl3}, together with an evaluation of the suitability of these newly created lines to study cone-specific disease mechanisms.

Methods

Animal Models and Genotyping

All mice were group housed in a climate-controlled facility on a 12-hour light/dark cycle with food and water ad libitum. All experiments were approved by the University of Western Australia and Harry Perkins Medical Institute's Institutional Animal Care and Use Committees, and conducted in accordance with the ARVO Statement for the Use of Animals in Ophthalmic and Vision Research. The Chrnb4.EGFP mouse strain (STOCK Tg(Chrnb4-EGFP)CL200Gsat/Mmnc, RRID:MMRRC_000259-UNC), was obtained from the Mutant Mouse Resource and Research Center (MMRRC) at the University of North Carolina at Chapel Hill, an National Institutes of Health–funded strain repository, and was donated to the MMRRC by Nathaniel Heintz, PhD, of the Rockefeller University, GENSAT.[22] Two cone degeneration mouse models of achromatopsia were used in this study: *Gnat2*$^{cpfl3/cpfl3}$, a mild symptomatic, late onset cone disorder (JAX stock #006795; B6.ALS-*Gnat2*^{cpfl3}/Boc),[27] and *Pde6c*$^{cpfl1/cpf11}$ (JAX stock #003678; B6.CXB1-*Pde6c*^{cpfl1}/J),[26,28] a severe, early onset cone degeneration.[29] Both lines were obtained from the Jackson Laboratory (Bar Harbor, ME). The Chrnb4.GFP (EGFP is referred to as GFP only from here on) was subsequently crossed with both cone degeneration models to produce the novel mouse lines designated *Gnat2*$^{cpfl3/cpfl3}$.GFP and *Pde6c*$^{cpfl1/cpf11}$.GFP (referred to as *Gnat2*.GFP and *Pde6c*.GFP from here on). All three lines were then backcrossed on to a C57BL/6J background for 8 generations. Genotyping for all lines was outsourced to TransnetYX (Cordova, TN).

Tissue Processing and Immunohistochemistry

Immunohistochemistry and terminal deoxynucleotidyl transferase dUTP nick-end labelling (TUNEL) processing and analysis were performed according to previously published protocols.[30] Briefly, eyes were collected from all lines at different ages indicated in the figures and fixed in 4% paraformaldehyde (Electron Microscopy Slides, 15710) for 1 hour on ice. Cornea and lens were then dissected out and eyes incubated in 4% paraformaldehyde for another 1 hour on ice. They were then incubated in 20% sucrose overnight at 4°C. The following day eyes were frozen in optimal cutting temperature compound (Tissue-Tek O.C.T. Compound, Emgrid, Australia) and stored at −20°C before sectioning. Retinal sections were collected on superforst slides (Hurst, Australia) and cut using a Leica (Wetzlar, Germany) Cryostat CM3050 at 14 µm. For immunohistochemical staining, slides were blocked for 1hour in blocking solution (1% w/v bovine serum albumin [Bovogen Biologicals, BSAS0.1, Keilor East, Australia], 0.5% v/v Triton-X-100 [LabChem, 1552-500Ml, Zelienople, PA], 5% v/v normal goat serum [Sigma-Aldrich, G9023, St Louis, MO], 1× phosphate-buffered saline [PBS]) at room temperature then incubated overnight at 4°C with primary antibody diluted in blocking solution. The following day, slides were washed in 1× PBS and incubated for 2 hours at room temperature with Alexa-Fluor 546 conjugated secondary antibody (1:500). For GFP only staining, the secondary antibody incubation was not necessary as the anti-GFP primary was already conjugated. Slides were then washed in 1× PBS several times, incubated in 4′,6-diamidino-2-phenylindole (1:1000, Sigma-Aldrich, D9542-5MG) solution for 5 minutes, mounted using fluorescent mounting media (DAKO, Glostrup, Denmark) and allowed to dry at room temperature before imaging. Primary antibodies used include rabbit anti-cone arrestin, (Arr3, 1:1000, Millipore AB15282, Billerica, MA) and rabbit anti-GFP Alexa Fluor 488 conjugated (1:500, Invitrogen, Carlsbad, CA; #A-2131); and secondary antibody Goat Anti-Rabbit IgG H&L Alexa Fluor 568 (1:500, Abcam, Cambridge, UK; ab175471). Retinal wholemounts for CD45 and collagen IV staining followed a previously published protocol.[31] Image acquisition was done on a Nikon A1Si confocal microscope and images captured on an Andor 885 EMCCD camera with the NIS Elements imaging software.

RNA Extraction, Reverse Transcription, and Quantitative Real-Time PCR (qPCR)

Total RNA was extracted from whole retinas using TriReagent (Sigma-Aldrich) as per manufacturer's instructions. Reverse transcription was performed using QuantiTect Reverse Transcription Kit (Qiagen, Hilden, Germany) as per manufacturer's

instructions. The qPCR was performed on a Bio-Rad CFX Connect Real-Time System using Taqman Fast Advanced mastermix (ThermoFisher, Waltham, MA) with the following gene assays: *Arr3*, Mm00504628_m1; *Chrnb4*, Mm01179558_m1; *Cnga3*, Mm00802288_m1; *Gapdh*, Mm99999915_g1; *GFP*, Mr04097229_mr; *Gnat2*, Mm00492394_m1; *Opn1mw*, Mm00433560_m1; and *Pde6c*, Mm00473920_m1. Gene expression was normalized to *Gapdh* and relative expression calculated using the $\Delta\Delta$Ct method.[32]

Electroretinogram (ERG)

Retinal function was evaluated via full-field flash scotopic and photopic ERG recordings using the HMsERG system (OcuScience LLC, Rolla, MO). Mice were dark adapted overnight and handled subsequently only under dim red light. Mice were anaesthetized with isoflurane and pupils dilated by applying 1% tropicamide (MYDRIACYL; Alcon, Geneva, Switzerland) to the surface of the cornea. A drop of 2% Hypromellose (GONIOVISC, HUB Pharmaceuticals, LLC, Rancho Cucamonga, CA) solution was also applied to the cornea to keep it moist throughout the recordings. Sedated animals were placed on a heating pad kept at 37°C and a stainless steel ground electrode was placed subdermally above the base of the tail and reference electrodes were placed subdermally in each cheek along the jaw line in an anterior direction. The eye electrodes combined a silver thread with a contact lens and was placed on top of the cornea for each eye. The mice was then placed under the Ganzfeld dome to ensure a uniform illumination stimulus was presented.[30]

For scotopic recordings animals were dark adapted for 8 to 12 hours and a dark-adapted single-flash intensity series was obtained through presentation of 1ms flashes with the following intensities (all in cd.s.m^{-2}): 0.1, 0.3, 1, 3, 10, and 25. The time interval between consecutive flashes and the number of times the stimulus was repeated (for subsequent averaging) was 10 seconds and four repeats at 0.10 Hz. Recovery time between different intensities was 60 seconds. Photopic recordings were obtained on a different day therefore animals had not been dark adapted. Following a 10-minute light adaptation at 30 cd.m^{-2}, a series of flashes on a 30 cd.m^{-2} background was presented at 2 Hz of the following intensities (all in cd.s.m^{-2}): 0.01, 0.03, 0.1, 0.3, 1, 3, 10, and 25. The time interval between consecutive flashes and the number of times the stimulus was repeated (for subsequent averaging) was 0.5 seconds and 32 repeats. Before analysis of b- and a-waves, a lowpass 150-Hz filtering was applied and data were analyzed using the ERGView Software (4.380R; OcuScience LLC) and Excel (Microsoft, Redmond, WA).

Cell Dissociation and Flow Cytometry Analysis

Three different proteolytic enzymes were initially assessed for retinal cell dissociation on 2-month-old *Gnat2*.GFP mouse retinas (Papain: LK003176, Worthington Biochemicals, Lakewood, NJ; Trypsin type XI: T1005, Sigma-Aldrich; Liberase: 5401119001, Roche, Basel, Switzerland). Each enzyme was tested in three independent experimental repeats (minimum of $n = 3$ per repeat) conducted on different days. Data from 6-month-old mouse retinas for average GFP$^+$ cell quantification were obtained after the papain dissociation protocol (minimum of $n = 5$ per mouse line). The trypsin and liberase protocols were taken from previously published studies,[31,33,34] while the papain protocol was adapted from Barber et al[35] as follows. Freshly dissected retinal sample were incubated in a 1:20 solution of papain/DNase (Worthington Biochemicals, LK003176/LK003170) at 37°C for 45min and gently triturated. The solution was spun for 5 minutes at 150×g, supernatant discarded and the pellet washed twice in Earle's balanced salt solution (Gibco, Grand Isle, NY; 24010-043), spun and supernatant discarded. The pellet was resuspended in Earle's balanced salt solution containing 9.5%v/v Ovomucoid Protease Inhibitor and 5%v/v DNase (LK003182/LK003170, Worthington Biochemicals) and incubated at 37°C for 10 minutes. The sample was pelleted again before resuspension in Earle's balanced salt solution with 10%v/v DNase. Samples were incubated with propidium iodide (PI; 1:1000 dilution; P4170, Sigma-Aldrich) on ice for 30 minutes, and then washed in fluorescent activated cell sorting (FACS) buffer (2% heat-inactivated fetal calf serum [Fisher Biotec, Webley WA, Australia], 1 mM EDTA, 1× PBS), pelleted, and resuspended in FACS buffer. Flow cytometry analysis was performed on a BD FACSAria II or a BD FACSCanto II (Becton Dickson) and FACS was performed on a BD FACSMelody.

Statistical Analysis

Statistical analysis was performed in GraphPad PRISM software. The Student t-test or two-way analyses of variance were used to identify statistical significance ($P < 0.05$), using Bonferroni's post hoc test where applicable. All data represented are represented as the mean ± standard error of the mean.

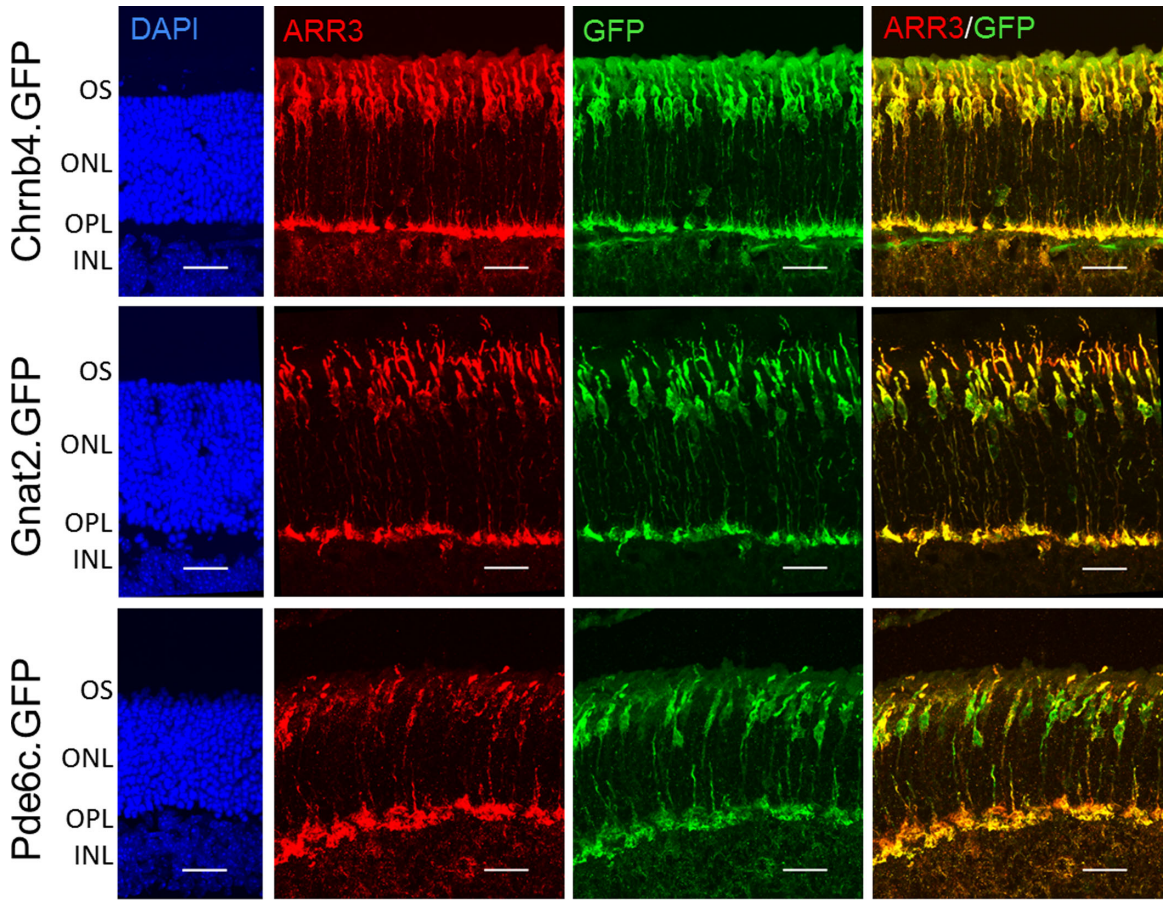

Figure 1. GFP expression is localised to cone photoreceptors. Shown are representative confocal images of retinal cryosections of Chrnb4.GFP, *Gnat2*.GFP, and *Pde6c*.GFP mice at P24. The 4′,6-diamidino-2-phenylindole (DAPI; *blue*) nuclear stain shows the retinal layers. Immunohistochemical detection of cone arrestin (ARR3, *red*) and GFP (*green*) shows co-localization in cone photoreceptors (yellow, rightmost column). INL, inner nuclear layer; ONL, outer nuclear layer OPL; outer plexiform layer; OS, outer segment. Scale bar = 20 µm.

Results

Retinal GFP Expression Is Exclusively Localized to Cone Photoreceptors

Our genotyping results showed that, in all three lines, the *GFP* allele was only present in a heterozygote state, suggesting that homozygosity is most likely embryonically lethal (data not shown). To confirm and validate the expression of GFP exclusively in cone photoreceptors in the newly crossed *Pde6c*.GFP and *Gnat2*.GFP lines, retinal cryosections were stained for the cone-specific cell marker cone arrestin (Arr3) (Fig. 1). The endogenous expression of GFP in the transgenic lines was low, requiring a GFP antibody for stronger visual detection through immunohistochemistry. As shown in postnatal day 24 (P24) Chrnb4.GFP retina (Fig. 1), cone photoreceptors were aligned along the apical edge of the outer nuclear layer (ONL), facing away from the vitreous cavity. Expression of both cone arrestin (Arr3) and GFP was seen throughout the length of the cone cells, including the outer segments, cell bodies and synapse terminals. This pattern of staining was also noted in *Gnat2*.GFP and *Pde6c*.GFP P24 retinas (Fig. 1). As expected, and in line with previous reports for these mouse lines,[26,28,36] there was an observed disorganization of cone photoreceptors in both of the novel transgenic achromatopsia mouse models, as well as reduced Arr3 fluorescence in the cell bodies. This observed phenotype was found to be more severe in the *Pde6c*.GFP line, correlating with previous studies in the original $Pde6c^{cpfl1}$ mouse line.[36]

GFP Expression Does Not Affect Cone Cell Function

To ensure GFP expression did not have a detrimental impact on visual function, electroretinogram

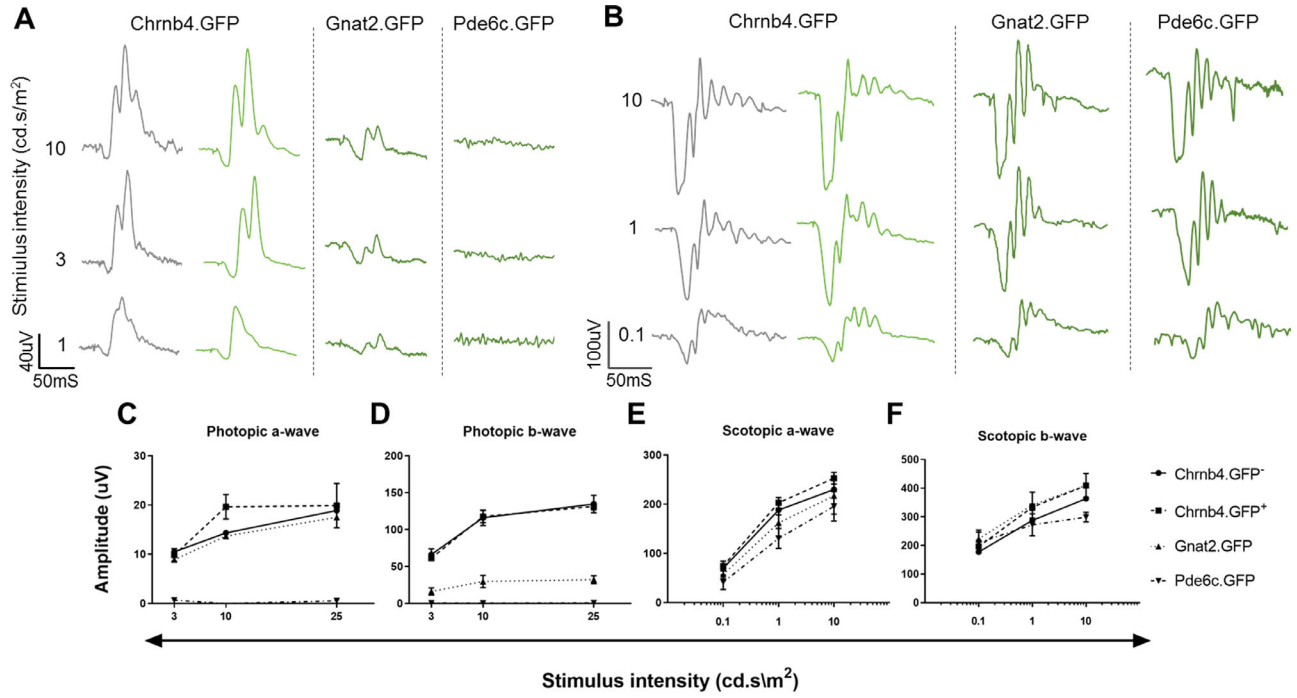

Figure 2. Functional analysis via ERG on all mouse lines at various stimulus intensities. (A) Photopic ERG traces of Chrnb4 GFP$^-$ (*grey*) and GFP$^+$ (*light green*) mice as well as *Gnat2*.GFP and *Pde6c*.GFP mice showing no difference between Chrnb4 GFP$^-$ and GFP$^+$ mice but a decrease in response in the *Gnat2*.GFP and *Pde6c*.GFP lines. (B) Scotopic ERG traces Chrnb4 GFP$^-$ (*grey*) and GFP$^+$ (*light green*) mice as well as *Gnat2*.GFP and *Pde6c*.GFP mice showing similar responses between all lines. (C, D) Quantification of photopic a- and b-wave responses for all mouse lines, except *Pde6c*.GFP which was omitted due to no detectable response. (E, F) Quantification of scotopic a- and b-wave responses for all mouse lines. $n = 3$–4 for each mouse line. Values are mean ± standard error of the mean.

(ERG) recordings were performed on Chrnb4.GFP, *Gnat2*.GFP, and *Pde6c*.GFP mice at P60 (Fig. 2). Figure 2A shows the average traces ($n \geq 3$) of the photopic and scotopic response for each line. There were no significant differences in photopic and scotopic responses between Chrnb4 GFP$^+$ and GFP$^-$ mice (Figs. 2A, B). Scotopic responses of the *Gnat2*.GFP and *Pde6c*.GFP lines revealed no statistical significance compared with Chrnb4.GFP, but a slightly lower b-wave response at the 10 cd.s/m^2 intensity for the *Pde6c*.GFP was observed, as seen in previous studies (Fig. 2F)[37]. Photopic responses (Fig. 2A) were not measurable for the *Pde6c*.GFP line but a diminished response was recorded in the *Gnat2*.GFP line. Both these results are consistent with previous reports on these lines.[26,27]

GFP Expression Does Not Affect Cell Survival or Cone Biology, But Decreases with Age

Next we determined if expression of GFP driven by the *Chrnb4* promoter affected cone cell health/survival or molecular function. Cell death in the ONL of P24 Chrnb4.GFP mice was identified by TUNEL staining and revealed no difference between GFP$^+$ and GFP$^-$ retinas (Figs. 3A, B). Due to the harsh nature of the membrane permeabilization steps required in the TUNEL assay, GFP visualization was not possible. Thus, we are unable to separate cone versus rod death in the ONL. However, the number of TUNEL$^+$ cells localized within the most apical section of the ONL (where cone cell bodies are found) was not significant between GFP$^+$ and GFP$^-$ retinas ($P = 0.133$, data not shown). Further, qPCR data showed no significant difference between P24 GFP$^+$ and GFP$^-$ retinas in the expression of cone-specific genes (*Gnat2*, *Pde6c*, *Cnga3*, *Arr3*, and *Opn1mw*) (Fig. 3C). To evaluate if sustained expression of GFP could generate an inflammatory response, retinal wholemounts from P60 GFP$^+$ and GFP$^-$ Chrnb4.GFP mice were co-stained with the pan leukocyte anti-CD45 marker and the anti-collagen IV antibody to visualize blood vessels. As shown in Figure 3D, CD45$^+$ cells were only found within retinal vessels in both genotypes, indicating that the presence of GFP does not elicit leukocyte cell infiltration within the retina.

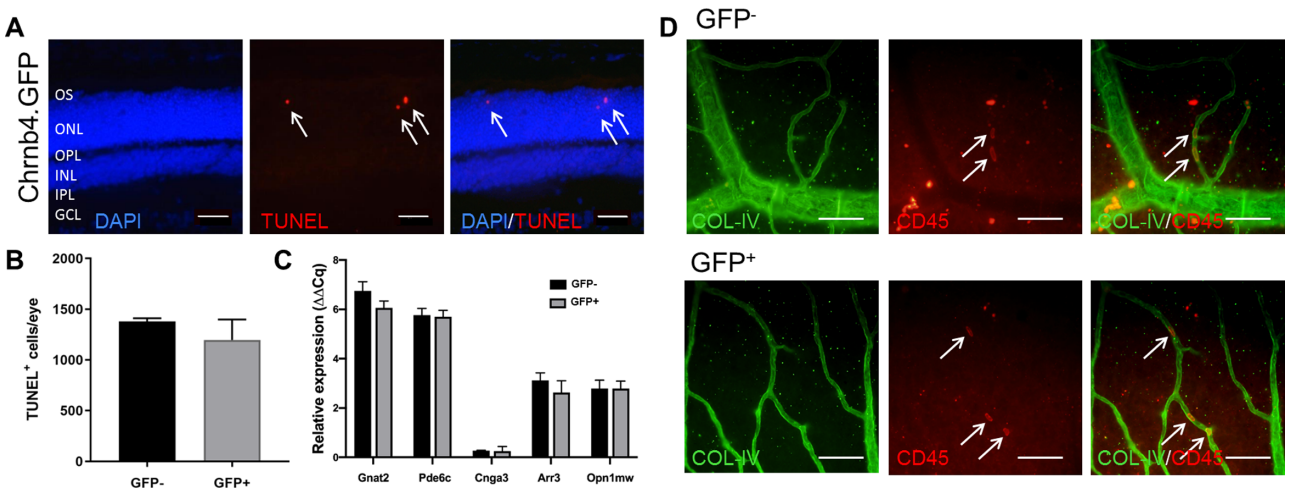

Figure 3. Characterization of Chrnb4.GFP and the effect of GFP expression on cone and retinal biology. (A) Representative confocal images of immunohistochemical staining of a P24 Chrnb4.GFP retina showing TUNEL$^+$ cells in the ONL. *White arrows* indicate TUNEL$^+$ labelled cells. Scale bar = 50 µm. (B) Graph showing the average number of TUNEL$^+$ cells counted in the ONL from GFP$^-$ and GFP$^+$ Chrnb4 retinas at P24. No significant difference was observed between genotypes. Values are mean ± standard error of the mean; GFP$^-$: 1379.8 ± 31.2; GFP$^+$: 1197.6 ± 201.5; n = 4/genotype. (C) Relative gene expression of cone-specific markers show no significant difference between GFP$^-$ and GFP$^+$ Chrnb4 mice. Each bar represents the relative expression calculated by the ΔΔCt method normalized to *Gapdh*. Values are mean ± standard error of the mean; n = 3/genotype. (D) Representative confocal images of immunohistochemical staining of collagen IV (COL-IV; *green*) and CD45$^+$ (*red*) in GFP$^-$ and GFP$^+$ Chrnb4 retinas at P60. CD45$^+$ cells were found only within blood vessels and are indicated by white arrows. Upper images, scale bar = 50 µm; lower images, scale bar = 100 µm.

To evaluate the temporal expression of GFP at the protein and messenger RNA level, immunohistochemical staining and qPCR were performed at P12, P24, P32, P40, P60, P90, and 8 months of age (n = 3 at each age) (Fig. 4 and Supplementary Fig. 1). There was a strong GFP signal at P12 (Fig. 4A), which diminished with age; in 8-month-old retinas, the GFP signal was only detected with much brighter imaging settings and not present in all cone cells (Supplementary Fig. 1). At the messenger RNA level, GFP was most highly expressed at P12, and showed a significant decrease with age until P40 ($P < 0.05$, Fig. 4C), where GFP expression plateaued. To determine if the decline of GFP expression was driven by decreased expression of the *Chrnb4* promoter over time, expression of *Chrnb4* was assayed. As shown in Figure 3D, there was a temporal decrease in *Chrnb4* expression with age, with a significant decrease between P32 and P40 ($P = 0.03$).

GFP Is a Reliable Marker for Identifying and Isolating Cone Cells Regardless of Age

Despite the observed decrease in GFP expression over time, we nevertheless wanted to evaluate the efficacy of a more sensitive method such as flow cytometry, for cone detection. We initially examined three proteolytic enzymes commonly used in tissue dissociation to determine the optimal enzymatic digest protocol and sensitivity as defined by the number of GFP$^+$ cones from one of our disease models, the *Gnat2*.GFP, tested at a stage where GFP expression is low but still mostly present (P60). The three enzymes tested (papain, trypsin, and liberase) showed varying degrees of efficiency, but papain dissociation resulted in significantly more GFP$^+$ cells (Figs. 5A–E; $P < 0.003$) and a significantly lower percentage of dead cells (27%; $P < 0.05$). The liberase and trypsin protocols had a similar percentage of dead cells (44% and 46%, respectively), but the liberase protocol generated the lowest number of GFP$^+$ cells (Fig. 5E), a loss of defined cell populations (Fig. 5A), and an observed change in morphology of GFP$^+$ cones (Fig. 5C). We then investigated the sensitivity of flow cytometry to detect GFP$^+$ cones at a later time point when GFP expression was shown to have decreased further. We were able to demonstrate that GFP$^+$ cones can still be detected at this age, and the difference in cone numbers between Chrnb4.GFP, *Gnat2*.GFP, and *Pde6c*.GFP is shown in Figure 5F. Relative to Chrnb4.GFP, *Pde6c*.GFP and *Gnat2*.GFP retinas showed a significant 85% (15.6 ± 6.2%; $P = 0.005$) and 44% (66.6 ± 15.6%; $P = 0.228$) decreases in cone numbers, respectively.

After defining the optimal dissociation protocol for flow cytometry of GFP$^+$ cones, we evaluated the

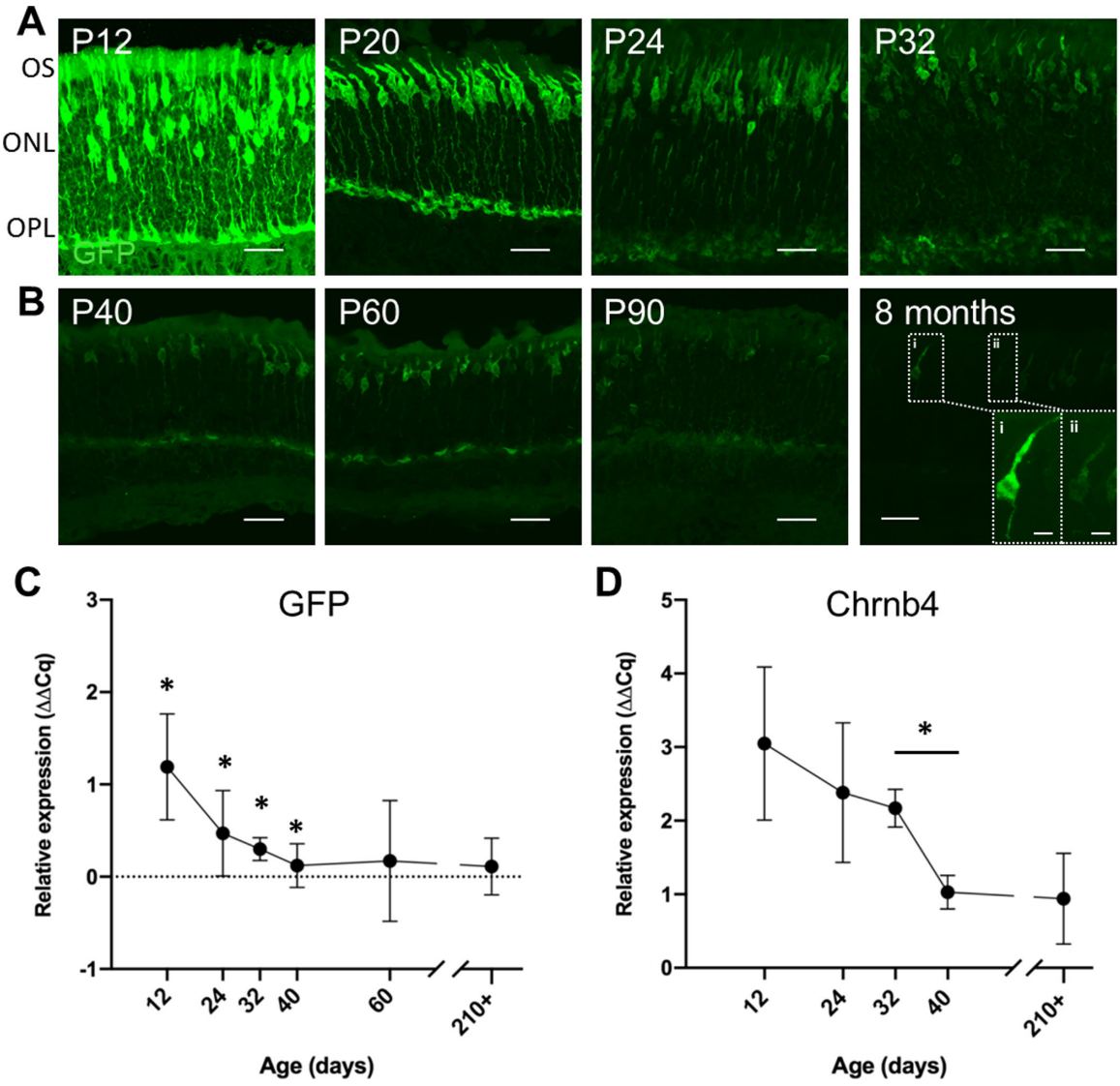

Figure 4. Temporal decrease in GFP expression in Chrnb4.GFP mice with age. (A, B) Representative confocal images of retinal cryosections in Chrnb4.GFP mice show a decrease in GFP fluorescence over time. Scale bars = 20 µm. (i, ii) The 8 months panel shows two individual cones at higher magnification with images modified to account for lower expression levels highlighting the intercellular GFP expression differences. Scale bars = 5 µm. (C) A qPCR analysis of *GFP* expression shows a temporal decrease of *GFP* with age, where highest *GFP* expression was measured at P12 time point with significant decreases until the P40 time point. Asterisks denote time points where *GFP* expression was significantly decreased ($P < 0.05$) compared with P12. (D) A qPCR analysis of *Chrnb4* gene expression also shows a temporal decrease over time, with a significant decrease in expression between time points P32 and P40 ($P = 0.03$, unpaired two-tailed Student *t*-test). All qPCR analyses were normalized to *Gapdh*, $n = 3$ for each time point. Values are mean ± standard error of the mean.

potential of using the new GFP$^+$ achromatopsia lines for isolating a pure cone population using FACS for single cell applications. Figure 5G shows the representative scatter plots of the cell gating strategy used to sort a highly enriched cone population from two P24 *Gnat2*.GFP retinas. Single cell sorting was done on all three lines and post-sort analyses showed a consistent 90% to 95% purity in the sorted cell populations (Fig. 5G).

Discussion

GFP is an extremely versatile biomarker; it has been used extensively in different species and tissue types to identify and track various cell populations.[38,39] For the study of scarce cell populations, such as cone photoreceptors, the visualization, identification, and ability to isolate them from other retinal cell types is

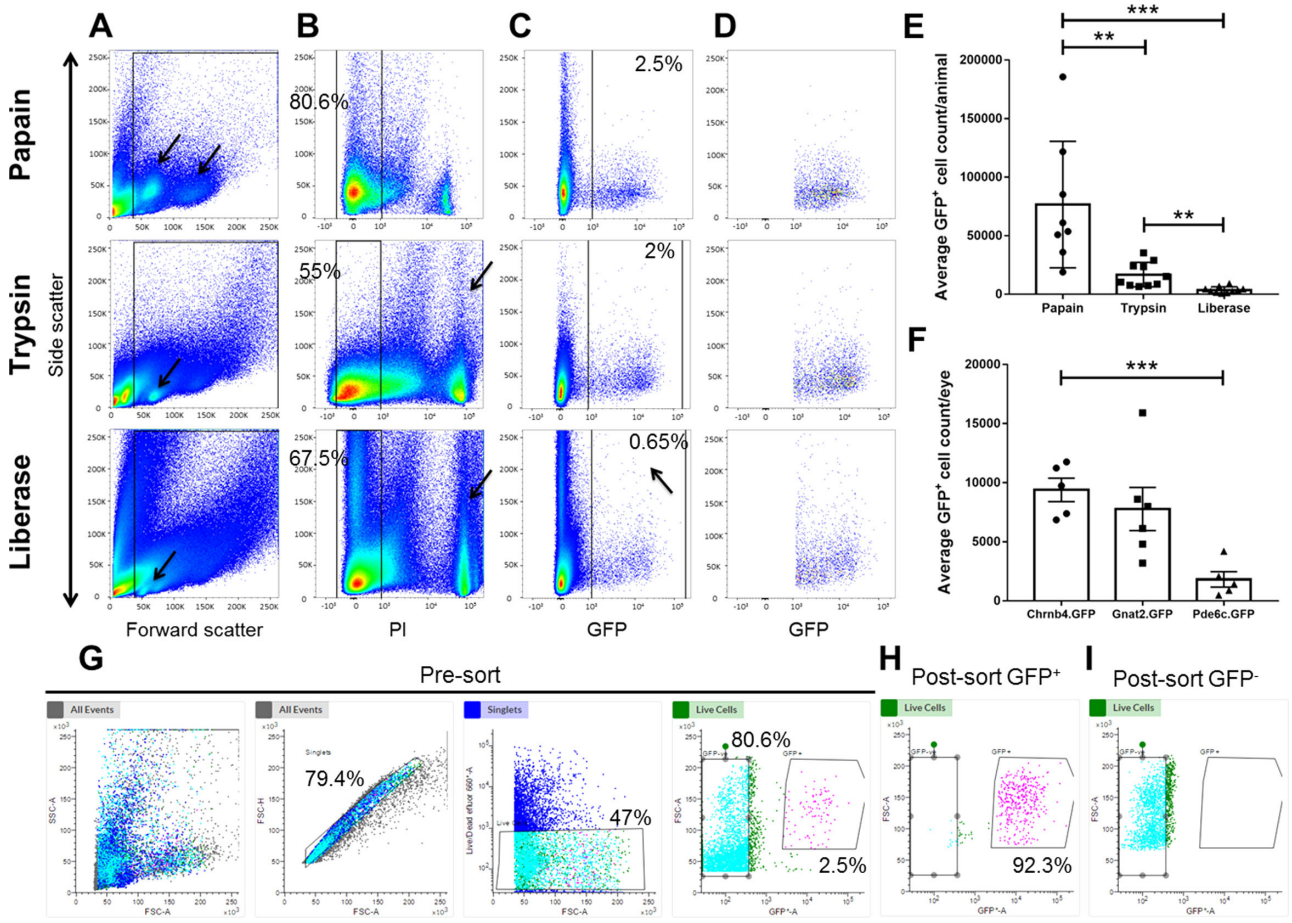

Figure 5. Flow cytometry validation for cone degeneration GFP$^+$ lines. (A–D) Flow cytometry scatter plots of cell gating strategy. Retinas from *Gnat2*.GFP P60 animals were used for testing different retinal cell dissociation methods. (A) Representative gating of all cells. (B) Representative gating of live cells. (C) Representative gating of GFP$^+$ cells. (D) The resulting GFP$^+$ population. (E) Average GFP$^+$ cell counts from flow cytometry data show significantly higher numbers of GFP$^+$ cells from the papain protocol. (F) Average GFP$^+$ cell counts from flow cytometry data show significantly lower number of GFP$^+$ cells in the *Pde6c*.GFP line compared with the Chrnb4.GFP line at 6 months of age. Values are mean ± standard error of the mean. ***$P = 0.0006$, **$P = 0.003$, and *$P = 0.001$ (unpaired two-tailed Student *t*-test). (G–I) Representative single cell fluorescent activated cell sort (FACS) cone cell gating strategy from a P24 *Gnat2*.GFP retina. Post-sort purity analysis on the (H) GFP$^+$ sorted cone cells is shown alongside the post-sort analysis of the (I) GFP$^-$ cells from the same retina.

important in advancing our understanding of their function, for example, for use in single cell transcriptome sequencing.[40] Although the expression of an exogenous protein has the potential to disrupt molecular and celular functions of the cell in which it is expressed, as noted with some fluorescent markers (e.g., dsRed),[41] GFP expression is well-tolerated in photoreceptors, with no deleterious effect on morphology or function.[42–44] Our data support this conclusion as no adverse effects of Chrnb4-driven GFP expression were found on cone viability, gene expression, immune system activity, or visual function, further validating the use of the Chrnb4.GFP line as a powerful tool to study cone biology in health and disease.

The characterization of cone function and biology has been hampered by a lack of suitable transgenic reporter lines or reliable cell markers that identify cone cells or cone lineage. The use of the *Chrnb4* promoter is unique in its ability to direct retinal GFP expression exclusively in cone photoreceptors. Further, it expresses GFP in all cone subtypes, as evidenced by co-localization with the pan-cone staining marker cone arrestin. This strategy circumvents issues associated with using cone subtype-specific promoters, such as the one used in the transgenic OPN1LW-EGFP mouse, where the human *OPN1LW* promoter was used to target GFP expression mainly to M cones.[44–46] Furthermore, the suitability of this transgenic mouse line was seriously questioned when it was shown that the OPN1LW-GFP transgene integration site falls within a chromosomal region associated with dominant cone dystrophies (MCDR1 and PBCRA

locus),[47,48] inducing an age-related cone degeneration phenotype in these mice.[44,46]

Several cone-targeted transgenic mouse lines now exist; however, GFP expression is observed in multiple cell types. Crx-GFP identifies both rods and cones[49] and both Ccdc136-GFP and Lhx4-GFP lines target cone and bipolar cells.[40,50] In contrast, the Chrnb4.GFP transgenic line is the only line in which cones are selectively targeted and several studies have now used it in examination of retinal cell-specific transcriptomes,[23] cone development after transplantation,[24] and the involvement of microRNAs in cone survival.[25] The present study further validates the use of the Chrnb4.GFP line as the most reliable cone reporter mouse model currently available, albeit limited. From our present data with two mouse models of achromatopsia, we show that GFP expression in young retinas to be independent from disease progression. This contrasts with the expression/staining of other cone specific markers (including opsins,[25] arrestin,[51] and peanut agglutinin),[52] which are lost during disease progression, thus limiting their usefulness as disease-independent markers. The presence of GFP throughout the cone cell could also facilitate a more focused investigations during cone degeneration including synapse remodeling, outer segment breakdown and cone migration, which have been historically difficult to study due to expression variability during diseased states. We therefore believe that backcrossing disease models to the Chrnb4.GFP line can be an extremely efficient way to study early cone degeneration.

Age-Specific Limitations

Although the use of the Chrnb4.GFP mouse has produced promising results for cone photoreceptor investigations, limitations arise as GFP fluorescence is low and requires a GFP antibody for visual detection. As such, the low endogenous GFP expression precludes the use of in vivo visualization techniques such as fundus and OCT imaging. The temporal progression of GFP expression investigated in the Chrnb4.GFP line from P12 showed an age-dependent decrease in both gene and protein expression. However, GFP fluorescence was still detectable as late as 6 months via flow cytometry. The decrease in GFP expression we report coincides with a decline in *Chrnb4* expression, indicating that the loss of GFP^+ cones with age is most likely linked to an endogenous decrease of *Chrnb4* expression and not to a potential age-related loss of cones. Previous studies have shown conflicting data on cone loss and aging, with no change in cone numbers up to 2 years, despite a consensus on cone function declining with age.[53–55] In contrast, a more recent in-depth histologic analysis showed a 18% decrease in cone numbers at 12 months, more specifically in the ventral retina and focused on M-opsin cones.[56] Our histologic data show that with age, GFP expression levels per individual cone is decreasing, and the reduced number of visually identified GFP^+ cones indicates that some cones have lost GFP expression completely. Based on the data from these previous studies[53–56], the potential cone loss within the time points analyzed in this study would be no more than 18%, suggesting that the loss of GFP expression seen with age is linked to the decreased activity of the *Chrnb4* promoter and not to cone loss. It remains to be determined if the age-related GFP loss affects S- and M-cones differently as this was not investigated in this study. Future studies using these transgenic GFP mouse lines could encompass earlier time points with confidence, although, their use in studies involving age-related conditions (such as age-related macular degeneration), and IRDs models with later onset, might be limited due to the temporal decrease of GFP expression.

Future Applications of GFP Lines

The presence of GFP-expressing cones in mouse models of cone dystrophy such as achromatopsia will provide a substantial aid in the research of effective therapies for these conditions. The novel *Gnat2*.GFP and *Pde6c*.GFP achromatopsia mouse lines created for this study can now provide a more sensitive and reliable tool to investigate the effects of disease-causing mutations on cone photoreceptors and may be broadened to look at cone biology, disease mechanisms and drug discovery. Disease mechanisms can also be studied at the molecular level using techniques such as transcriptome analysis, where identification of potential markers can help in targeting drug therapy treatments. Our data show that isolating a pure cone population is feasible: single cones can be accurately sorted from the rest of the retinal cell population with a 90% to 95% accuracy, similar to data previously shown by Siegert et al 2012.[23] The previous inability, due to the lack of reliable cell surface markers, to reliably isolate mouse cones from the remaining retinal population, has hampered previous attempts to study cone biology in more detail. Our data showed significant enzyme-specific differences, with the papain-based protocol producing the greatest number of live cones. Therefore careful consideration should be taken when selecting the appropriate protocol for the use of these novel lines for flow analysis and its downstream

applications. Despite of their limitations, using these lines for preclinical validation of cone-directed treatments could potentially offer more reliable and accurate data which would accelerate the clinical translation of future treatments.

Final Conclusions

Because cones are the cells responsible for bright light and color vision detection, it is imperative that we understand how these cells are affected in different types of vision loss conditions and what can be done to halt cell death and/or to improve survival rates. However, understanding the molecular mechanisms behind cone loss has lagged behind the genetic dissection of IRDs. This knowledge gap has impeded the development of effective treatment strategies that are strategically focused on preserving cone-mediated vision. The results presented in this study offer an in-depth validation of fluorescent mouse models as a tool to study cone biology in health and vision loss conditions. The novel achromatopsia mouse models validated in this study, *Gnat2*.GFP and *Pde6c*.GFP, could provide a useful tool to investigate the cellular and molecular mechanisms of cone dysfunction, and where future studies may be able to more accurately investigate the functional defects and molecular changes in cone photoreceptors associated with mutations in the *Gnat2* and *Pde6c* genes.

Acknowledgments

Supported by an Australian Research Council Discovery Early Career Research Award DE140100320 (LSC); a 2016 Retinal Australia Research Grant (LSC); a 2018 grant from the Lindsay & Heather Payne Medical Research Charitable Foundation/Perpetual Impact Philanthropy Program (LSC).

The authors thank the facilities, and the scientific and technical assistance of Microscopy Australia at the Centre for Microscopy, Characterisation & Analysis, The University of Western Australia, a facility funded by the University, State and Commonwealth Governments.

Disclosure: **A.A. Brunet,** None; **P.I. Fuller-Carter,** None; **A.L. Miller,** None; **V. Voigt,** None; **S. Vasiliou,** None; **R. Rashwan,** None; **D.M. Hunt,** None; **L.S. Carvalho,** None

References

1. Crewe JM, Morlet N, Morgan WH, et al. Mortality and hospital morbidity of working-age blind. *Br J Ophthalmol*. 2013;97:1579–1585.
2. Daiger SPR B.J.F., Greenberg J., Christoffels A., Hide W. Data services and software for identifying genes and mutations causing retinal degeneration. *Invest Ophthalmol Vis Sci*. 1998;39:S295.
3. Berger W, Kloeckener-Gruissem B, Neidhardt J. The molecular basis of human retinal and vitreoretinal diseases. *Prog Retin Eye Res*. 2010;29:335–375.
4. Ortin-Martinez A, Nadal-Nicolas FM, Jimenez-Lopez M, et al. Number and distribution of mouse retinal cone photoreceptors: differences between an albino (Swiss) and a pigmented (C57/BL6) strain. *PLoS One*. 2014;9:e102392.
5. Fletcher EL, Jobling AI, Vessey KA, Luu C, Guymer RH, Baird PN. Animal models of retinal disease. *Prog Mol Biol Transl Sci*. 2011;100:211–286.
6. Carvalho LS, Vandenberghe LH. Understanding cone photoreceptor cell death in achromatopsia. *Adv Exp Med Biol*. 2016;854:231–236.
7. Kohl S, Hamel C. Clinical utility gene card for: achromatopsia - update 2013. *Eur J Hum Genet*. 2013;21.
8. Kohl S, Jagle H, Wissinger B, Zobor D. Achromatopsia. In: Adam MP, Ardinger HH, Pagon RA, et al. (eds), GeneReviews((R)). Seattle (WA); 1993.
9. Carroll J, Choi SS, Williams DR. In vivo imaging of the photoreceptor mosaic of a rod monochromat. *Vision Res*. 2008;48:2564–2568.
10. Dubis AM, Cooper RF, Aboshiha J, et al. Genotype-dependent variability in residual cone structure in achromatopsia: toward developing metrics for assessing cone health. *Invest Ophthalmol Vis Sci*. 2014;55:7303–7311.
11. Thomas MG, Kumar A, Kohl S, Proudlock FA, Gottlob I. High-resolution in vivo imaging in achromatopsia. *Ophthalmology*. 2011;118:882–887.
12. Sundaram V, Wilde C, Aboshiha J, et al. Retinal structure and function in achromatopsia: implications for gene therapy. *Ophthalmology*. 2014;121:234–245.
13. Thiadens AA, Roosing S, Collin RW, et al. Comprehensive analysis of the achromatopsia genes CNGA3 and CNGB3 in progressive cone dystrophy. *Ophthalmology*. 2010;117:825–830 e821.

14. Thomas MG, McLean RJ, Kohl S, Sheth V, Gottlob I. Early signs of longitudinal progressive cone photoreceptor degeneration in achromatopsia. *Br J Ophthalmol*. 2012;96:1232–1236.
15. Aboshiha J, Dubis AM, Cowing J, et al. A prospective longitudinal study of retinal structure and function in achromatopsia. *Invest Ophthalmol Vis Sci*. 2014;55:5733–5743.
16. Michaelides M, Aligianis IA, Holder GE, et al. Cone dystrophy phenotype associated with a frameshift mutation (M280fsX291) in the alpha-subunit of cone specific transducin (GNAT2). *Br J Ophthalmol*. 2003;87:1317–1320.
17. Thiadens AA, Somervuo V, van den Born LI, et al. Progressive loss of cones in achromatopsia: an imaging study using spectral-domain optical coherence tomography. *Invest Ophthalmol Vis Sci*. 2010;51:5952–5957.
18. Carvalho LS, Xu J, Pearson RA, et al. Long-term and age-dependent restoration of visual function in a mouse model of CNGB3-associated achromatopsia following gene therapy. *Hum Mol Genet*. 2011;20:3161–3175.
19. Komaromy AM, Alexander JJ, Rowlan JS, et al. Gene therapy rescues cone function in congenital achromatopsia. *Hum Mol Genet*. 2010;19:2581–2593.
20. Siegert S, Scherf BG, Del Punta K, Didkovsky N, Heintz N, Roska B. Genetic address book for retinal cell types. *Nat Neurosci*. 2009;12:1197–1204.
21. Heintz N. Gene Expression Nervous System Atlas (GENSAT). Nat Neurosci 7, 483 (2004), https://doi.org/10.1038/nn0504-483.
22. Gong S, Zheng C, Doughty ML, et al. A gene expression atlas of the central nervous system based on bacterial artificial chromosomes. *Nature*. 2003;425:917–925.
23. Siegert S, Cabuy E, Scherf BG, et al. Transcriptional code and disease map for adult retinal cell types. *Nature Neuroscience*. 2012;15:487–495.
24. Decembrini S, Martin C, Sennlaub F, et al. Cone genesis tracing by the Chrnb4-EGFP mouse line: evidences of cellular material fusion after cone precursor transplantation. *Mol Ther*. 2017;25:634–653.
25. Aldunate EZ, Di Foggia V, Di Marco F, et al. Conditional Dicer1 depletion using Chrnb4-Cre leads to cone cell death and impaired photopic vision. *Sci Rep*. 2019;9:2314. Published Feb 19, 2019, doi:10.1038/s41598-018-38294-9.
26. Chang B, Hawes NL, Hurd RE, Davisson MT, Nusinowitz S, Heckenlively JR. Retinal degeneration mutants in the mouse. *Vision Res*. 2002;42:517–525.
27. Chang B, Hawes NL, Hurd RE, et al. Mouse models of ocular diseases. *Vis Neurosci*. 2005;22:587–593.
28. Chang B, Grau T, Dangel S, et al. A homologous genetic basis of the murine cpfl1 mutant and human achromatopsia linked to mutations in the PDE6C gene. *Proc Natl Acad Sci USA*. 2009;106:19581–19586.
29. Fischer MD, Tanimoto N, Beck SC, et al. Structural and functional phenotyping in the cone-specific photoreceptor function loss 1 (cpfl1) mouse mutant - a model of cone dystrophies. *Adv Exp Med Biol*. 2010;664:593–599.
30. Hart NS, Mountford JK, Voigt V, et al. The role of the voltage-gated potassium channel proteins Kv8.2 and Kv2.1 in vision and retinal disease: insights from the study of mouse gene knockout mutations. *eneuro*. 2019;ENEURO.0032–0019.2019.
31. Voigt V, Andoniou CE, Schuster IS, et al. Cytomegalovirus establishes a latent reservoir and triggers long-lasting inflammation in the eye. *PLoS Pathog*. 2018;14:e1007040.
32. Livak KJ, Schmittgen TD. Analysis of relative gene expression data using real-time quantitative PCR and the 2(-Delta Delta C(T)) Method. *Methods*. 2001;25:402–408.
33. Samardzija M, Corna A, Gomez-Sintes R, et al. HDAC inhibition ameliorates cone survival in retinitis pigmentosa mice. *bioRxiv* 2019.12.13.874339; doi:10.1101/2019.12.13.874339.
34. Palfi A, Ader M, Kiang A-S, et al. RNAi-based suppression and replacement of rds-peripherin in retinal organotypic culture. *Human Mutation*. 2006;27:260–268.
35. Barber AC, Hippert C, Duran Y, et al. Repair of the degenerate retina by photoreceptor transplantation. *Proc Natl Acad Sci USA*. 2013;110:354–359.
36. Trifunovic D, Dengler K, Michalakis S, Zrenner E, Wissinger B, Paquet-Durand F. cGMP-dependent cone photoreceptor degeneration in the cpfl1 mouse retina. *J Comp Neurol*. 2010;518:3604–3617.
37. Lei B, Yao G, Zhang K, Hofeldt KJ, Chang B. Study of rod- and cone-driven oscillatory potentials in mice. *Invest Ophthalmol Vis Sci*. 2006;47:2732–2738.
38. Chudakov DM, Lukyanov S, Lukyanov KA. Fluorescent proteins as a toolkit for in vivo imaging. *Trends Biotechnol*. 2005;23:605–613.
39. Li Q, Timmers AM, Guy J, Pang J, Hauswirth WW. Cone-specific expression using a human red

opsin promoter in recombinant AAV. *Vis Res*. 2008;48:332–338.
40. Buenaventura DF, Corseri A, Emerson MM. Identification of genes with enriched expression in early developing mouse cone photoreceptors. *Invest Ophthalmol Vis Sci*. 2019;60:2787–2799.
41. Strack RL, Strongin DE, Bhattacharyya D, et al. A noncytotoxic DsRed variant for whole-cell labeling. *Nature Methods*. 2008;5:955–957.
42. Daniels DM, Shen WY, Constable IJ, Rakoczy PE. Quantitative model demonstrating that recombinant adeno-associated virus and green fluorescent protein are non-toxic to the rat retina. *Clin Exp Ophthalmol*. 2003;31:439–444.
43. Nour M, Quiambao AB, Al-Ubaidi MR, Naash MI. Absence of functional and structural abnormalities associated with expression of EGFP in the retina. *Invest Ophthalmol Vis Sci*. 2004;45:15–22.
44. Lipinski DM, Yusuf M, Barnard AR, et al. Characterization of a dominant cone degeneration in a green fluorescent protein-reporter mouse with disruption of loci associated with human dominant retinal dystrophy. *Invest Ophthalmol Vis Sci*. 2011;52:6617–6623.
45. Fei Y, Hughes TE. Transgenic expression of the jellyfish green fluorescent protein in the cone photoreceptors of the mouse. *Vis Neurosci*. 2001;18:615–623.
46. Beck SC, Schaeferhoff K, Michalakis S, et al. In vivo analysis of cone survival in mice. *Invest Ophthalmol Vis Sci*. 2010;51:493–497.
47. Gehrig A, Feibor U, Kelsell RE, Hunt DM, Maumenee IH, Weber BHF. Assessment of the interphotoreceptor matrix proteoglycan-1 (IMPG1) gene localised to 6q13-q15 in autosomal dominant Stargardt-like disease (ADSTGD), progressive bifocal chorioretinal atrophy (PBCRA), and North Carolina macular dystrophy (MCDR1). *J Med Genet*. 1998;35:641–645.
48. Small KW. North Carolina macular dystrophy: clinical features, genealogy, and genetic linkage analysis. San Francisco, CA: American Ophthalmological Society; 1998:925–961.
49. Samson M, Emerson MM, Cepko CL. Robust marking of photoreceptor cells and pinealocytes with several reporters under control of the *Crx*gene. *Dev Dynam*. 2009;238:3218–3225.
50. Smiley S, Nickerson PE, Comanita L, et al. Establishment of a cone photoreceptor transplantation platform based on a novel cone-GFP reporter mouse line. *Sci Rep*. 2016;6:1–15.
51. Gargini C, Novelli E, Piano I, Biagioni M, Strettoi E. Pattern of retinal morphological and functional decay in a light-inducible, rhodopsin mutant mouse. *Sci Rep*. 2017;7:5730.
52. Michalakis S, Geiger H, Haverkamp S, Hofmann F, Gerstner A, Biel M. Impaired opsin targeting and cone photoreceptor migration in the retina of mice lacking the cyclic nucleotide-gated channel CNGA3. *Invest Ophthalmol Vis Sci*. 2005;46:1516–1524.
53. Williams GA, Jacobs GH. Cone-based vision in the aging mouse. *Vision Res*. 2007;47:2037–2046.
54. Gresh J, Goletz PW, Crouch RK, Rohrer B. Structure-function analysis of rods and cones in juvenile, adult, and aged C57bl/6 and Balb/c mice. *Vis Neurosci*. 2003;20:211–220.
55. Li C, Cheng M, Yang H, Peachey NS, Naash MI. Age-related changes in the mouse outer retina. *Optom Vis Sci*. 2001;78:425–430.
56. Cunea A, Powner MB, Jeffery G. Death by color: differential cone loss in the aging mouse retina. *Neurobiol Aging*. 2014;35:2584–2591.